Published in final edited form as:
Cancer Res. 2011 May 15; 71(10): 3516–3527. doi:10.1158/0008-5472.CAN-10-3843.

Reprogramming CD19-specific T cells with IL-21 signaling can improve adoptive immunotherapy of B-lineage malignancies

Harjeet Singh[1], **Matthew J. Figliola**[1], **Margaret J. Dawson**[1], **Helen Huls**[1], **Simon Olivares**[1], **Kirsten Switzer**[1], **Tiejuan Mi**[1], **Sourindra Maiti**[1], **Partow Kebriaei**[2], **Dean A. Lee**[1,3], **Richard E. Champlin**[2], and **Laurence J.N. Cooper**[1,3]

[1]Division of Pediatrics, Children's Cancer Hospital, U.T. MD Anderson Cancer Center, Houston TX

[2]Department of Stem Cell Transplantation and Cellular Therapy, U.T. MD Anderson Cancer Center, Houston TX

[3]The University of Texas Graduate School of Biomedical Sciences at Houston, U.T. MD Anderson Cancer Center, Houston TX

Abstract

Improving the therapeutic efficacy of T cells expressing a chimeric antigen receptor (CAR) represents an important goal in efforts to control B-cell malignancies. Recently an intrinsic strategy has been developed to modify the CAR itself to improve T-cell signaling. Here we report a second extrinsic approach based on altering the culture milieu to numerically expand CAR^+ T cells with a desired phenotype. For, the addition of IL-21 to tissue culture improves CAR-dependent T-cell effector functions. We used electrotransfer of *Sleeping Beauty* (SB) system to introduce a CAR transposon and selectively propagate CAR^+ T cells on $CD19^+$ artificial antigen-presenting cells (aAPC). When IL-21 was present, there was preferential numeric expansion of CD19-specific T cells which lysed and produced IFN-γ in response to CD19. Populations of these numerically expanded CAR^+ T cells displayed an early memory surface phenotype characterized as $CD62L^+CD28^+$ and a transcriptional profile of naïve T cells. In contrast, T cells propagated with only exogenous IL-2 tended to result in an overgrowth of CD19-specific $CD4^+$ T cells. Furthermore, adoptive transfer of CAR^+ T cells cultured with IL-21 exhibited improved control of $CD19^+$ B-cell malignancy in mice. To provide coordinated signaling to propagate CAR^+ T cells, we developed a novel mutein of IL-21 bound to the cell surface of aAPC that replaced the need for soluble IL-21. Our findings demonstrate that IL-21 can provide an extrinsic reprogramming signal to generate desired CAR^+ T cells for effective immunotherapy.

Keywords

IL-21; CD19; Chimeric antigen receptor; T cell; artificial antigen presenting cells

INTRODUCTION

Adoptive transfer of antigen-specific T cells has been used to treat and prevent malignancies and opportunistic infections. To overcome immune tolerance to human tumor-associated antigens (TAAs), investigators have redirected specificity through the introduction of immunoreceptors. An initial clinical trial demonstrated the safety and feasibility of

Correspondence: Dr. Laurence J.N. Cooper, U.T. MD Anderson Cancer Center, Pediatrics - Research, Unit 907, 1515 Holcombe Blvd., Houston, TX 77030, Phone: (713) 563-3208; Fax: (713) 792-9832. ljncooper@mdanderson.org .

redirecting T-cell specificity to CD19, a TAA expressed on B-cell malignancies (1-3). These clinical data demonstrated that infused T cells were short lived due in part to the use of a 1st generation chimeric antigen receptor (CAR) that recognized CD19 independent of MHC via chimeric CD3-zeta (signal 1). In response, we developed a 2nd generation CD19-specific CAR to activate T cells through both CD3-ζ and CD28 endodomains (signal 1 and signal 2 respectively) to improve T-cell activation (4). To translate this CAR to clinical trials, we established a platform for non-viral gene transfer using the *Sleeping Beauty* (SB) system and subsequent selective expansion of CAR^+ T cells recursively co-cultured upon $CD19^+$ artificial antigen presenting cells (aAPC) modified from K562 to express CD19 and desired co-stimulatory molecules (5-7).

In addition to modifying the CAR itself to augment therapeutic potential, we have now manipulated the tissue culture environment to alter the types of CAR^+ T cells that can be generated. We investigated whether cytokines could be added to cultures to provide a "signal 3" to improve the CAR^+ T cells response to B-cell malignancies.

One attractive cytokine to use in the culturing of T cells is interleukin (IL)-21, which like IL-2, signals through the cytokine receptor common γ chain (IL-2Rγ). This was selected to be tested based on published work demonstrating that this cytokine increases tumor-specific T cells (8) and or, NK cells (9, 10) leading to anti-tumor immunity in animal models. Further, IL-21 provides a T-cell survival signal and can act in conjunction with CD28 to support proliferation and acquisition of effector functions (11). T cells genetically modified to have enforced secretion of IL-21 exhibited improved anti-tumor effect compared to T cells not modified to secrete cytokines (12). Recombinant soluble IL-21 has been intravenously administered in patients with metastatic renal cell carcinoma, melanoma, and lymphoma and anti-tumor activity has been observed (13). In contrast to IL-2, IL-21 also inhibits generation of human regulatory T cells *in vitro* (14).

We hypothesized that altering the culture environment by the addition of IL-21 will lead to improved numeric expansion and functionality of CD19-specific CAR^+ T cells. When IL-21 was present with or on aAPC, we found there was a preferential numeric expansion of CAR^+ T cells with a preference to propagate sub-populations of (i) $CD8^+$ T cells, (ii) memory T cells, and (iii) naïve T cells, which lysed and produced IFN-γ in response to CD19. This resulted in improved control of $CD19^+$ tumor in a mouse model of human T-cell immunotherapy.

MATERIAL AND METHODS

Plasmids

The SB transposon $_{CoOp}$CD19RCD28/pSBSO expresses the human codon optimized (CoOp) 2nd generation $_{CoOp}$CD19RCD28 CAR under human elongation factor 1-α (hEF-1α) promoter, flanked by the SB inverted repeats (6). To generate membrane bound IL-21 (mIL-21), the GM-CSF signal peptide sequence was directly fused to the coding sequence of mature human IL-21 which was attached via a modified [amino acid (aa) #108, Ser→Pro] 12 aa IgG4 hinge region (aa 99-110), to the 5′ end of a human immunoglobulin gamma-4 chain C_H2 and C_H3 regions (aa 111-327, UniProtKB#P01861), that was fused in frame to human CD4 transmembrane domain (aa 397-418, UniProtKB#P01730). After validating the sequence, the human codon optimized cDNA (GENEART) was cloned as a transposon into a SB expression plasmid, pT-MNDU3-eGFP (5) replacing the eGFP sequence to obtain $_{CoOp}$IL-21-Fc/pT-MNDU3 (Figure 6A). The SB transposase, SB11, is expressed *in cis* from the plasmid pCMV-SB11 (6).

Cell Lines and their propagation

Daudi co-expressing β_2-microglobulin (15) (Daudiβ_2m, a kind gift from Dr Brian Rabinovich, University of Texas MD Anderson Cancer Center, TX), NALM-6 (pre-B-cell, ATCC), U251T (glioblastoma; a kind gift from Dr Walder Debinksi, Wake Forest University, NC), CD19$^+$U251T (6) [expressing truncated CD19 ref, (16)] were cultured as described previously. NALM-6 cells were transduced using a MSCV based retroviral vector encoding enhanced firefly luciferase (effLuc) (17) fused with green fluorescent protein (GFP) (a kind gift from Dr Brian Rabinovich, MDACC, TX). Retrovirus was packaged as previously described (17), concentrated 50x using Amicon Ultra-15 100,000 NMWL centrifugal concentration units (Millipore, Billerica, MA), mixed with NALM-6 cells in the presence of 8μg/mL Polybrene (Sigma, St Louis, MS) and spinfected for 90 minutes at 2200 RPM/300C. One week later, GFP$^+$NALM-6 cells were sorted on a FACSAria cell sorter (BD Biosciences, San Jose, CA). Selective *in vitro* expansion of genetically modified T cells was performed using K562-derived aAPC (clone #4) co-expressing CD19, CD64, CD86, CD137L, and a membrane-bound IL-15 (mIL-15) (co-expressed with GFP) (15). Clone #4 was further modified to express mIL-21 using the construct $_{CoOp}$IL-21-Fc/pT-MNDU3. Briefly, 10^6 aAPC were re-suspended in 100 μL Amaxa Cell Line Nucleofector Solution V (Cat# VPA-1003) along with transposon ($_{CoOp}$IL-21-Fc/pT-MNDU3, 2 μg) and SB transposase (pCMV-SB11, 2 μg) DNA supercoiled plasmids, transferred to a cuvette and electroporated (Program T-16) using Nucleofector® II (Lonza, Switzerland). The transfectants were cultured for a week in complete media and a clone (D2) was obtained by plating at limited dilution after FACS-sorting. All cell lines were verified by morphology and/or flow cytometry, tested for *Mycoplasma*, and conserved in research cell bank on reception.

Generation of CAR$^+$ T cells

CD19-specific CAR$^+$ T cells were generated from PBMC using SB transposition as previously described and depicted in Figure 1 (5). Briefly, 10^7 to 2×10^7 mononuclear cells, isolated from blood by Ficoll-Paque density gradient centrifugation (GE Healthcare Bio-Sciences AB, Uppsala, Sweden), were re-suspended in 100 μL of Amaxa Nucleofector solution (Human T cell Kit, Cat# VPA-1002), along with CAR transposon (CD19RCD28/pSBSO, 15 μg) and SB transposase (pCMV-SB11, 5 μg) DNA plasmids, transferred to a single cuvette and electroporated (Program U-14) on day 0 using Nucleofector® II. The cells were rested for 2 to 3 hours at 37°C in incomplete phenol-free RPMI (HyClone, Logan, UT) and subsequently cultured overnight in phenol-free RPMI containing 10% FBS and stimulated the next day (day 1) with γ-irradiated (100 Gy) K562-aAPC at a 1:2 T cell/aAPC ratio. Additional γ-irradiated aAPC clone #4 were added every 7 days at the same ratio. When used, soluble recombinant human IL-21 (Cat# 34-8219-85, eBioscience, San Diego, CA) was added at a concentration of 30 ng/mL beginning the day after electroporation, and soluble recombinant human IL-2 (IL-2; Chiron, CA) was added to the cultures at 50 U/mL beginning 7 days after electroporation. For experiments where CAR$^+$ T cells were co-cultured on mIL-21$^+$ K562-aAPC (T cell/aAPC ratio 1:2), IL-2 (50U/mL) was added to the cultures on day 7 after electroporation. All exogenous cytokines continued to be supplemented on a Monday-Wednesday-Friday schedule for 7-day stimulation cycles marked by the addition of aAPC. The cultures were monitored by flow cytometry for the unwanted presence of a CD3^{neg}CD56$^+$ cell population and if the percentage exceeded approximately 10% of the total population, which usually occurred between 10-14 days of co-culture, a depletion for (CD3^{neg}) CD56$^+$ natural killer (NK) cells was performed using CD56 beads (Cat# 130-050-401, Miltenyi Biotech Inc., Auburn CA) on LS column (Cat# 130-042-401, Miltenyi Biotech Inc.) according to the manufacturer's instructions. T cells were enumerated every 7 days and viable cells counted based on Trypan blue exclusion using Cellometer automated cell counter (Auto T4 Cell Counter, Nexcelom Bioscience,

MA). At the time of electroporation and during the course of co-culture, programs "PBMC_human_frozen" and "Activated T cell" respectively, were used for counting cells on the Cellometer. The fold expansion (as compared to day 1) of: total, $CD3^+$, and CAR^+ cells at the end of 7, 14, 28 days of co-culture for individual experiments was calculated and the average compared between culture conditions using a Student's t-test.

Flow cytometry

Up-to-10^6 cells in 100μL volume were stained with fluorochrome-conjugated reagents which unless otherwise stated, were obtained from BD Biosciences (San Jose, CA): anti-CD3 FITC (Cat# 349201, 5μL), anti-CD3 PerCPCy5.5 (Cat# 340949, 4μL), anti-CD4 APC (Cat# 555349, 2.5μL), anti-CD8 PerCPCy5.5 (Cat# 341051, 4μL), anti-CD19 PE (Cat# 555413, 10μL), anti-CD28 PerCPCy5.5 (Cat# 337181, 4μL), anti-CD62L APC (Cat# 559772, 2.5μL), anti-CD45RA FITC (Cat# 555488, 5μL), anti-CD45RO APC (Cat# 559865, 2.5μL), anti-IL7Rα Alexa Fluor 647 (Cat# 558598, 10μL), anti-PD1 APC (Cat# 558694, 2.5μL), anti-PDL1 PE (Cat# 557924, 2.5μL), anti-NKG2D PE (Cat# 557940, 2.5μL), anti-Granzyme B Alexa Fluor 647 (Cat# 560212, 3μL), anti-Perforin PE (Reagent Set# 556437, 3μL), anti-HLA-ABC APC (Cat# 555555, 2.5μL), anti-CD86 PE (Cat# 555658, 2.5μL), anti-CD64 PE (Cat# 558592, 2.5μL), anti-CD137L PE (Cat# 559446, 2.5μL), anti-IFN-γ APC (Cat# 554702, 2μL), anti-pSTAT3 (pY705) PE (Cat# 612569, 20μL), anti-IL-21 PE (Cat# 12 7219-73, 2.5μL, eBiosciences), anti-CCR7 PE (Cat# FAB197P, 10μL, R&D Systems, Minneapolis, MN) and anti-CXCR4 PE (Cat# FAB173P, 10μL, R&D Systems). FITC-conjugated (Cat# H10101C, 3μL, Invitrogen, Carlsbad, CA) and PE-conjugated (Cat# H10104, 2.5μL, Invitrogen) $F(ab')_2$ fragment of goat anti-human Fcγ was used to detect cell surface expression of the CD19-specific CAR. Blocking of nonspecific antibody binding was achieved using FACS wash buffer (2% FBS and 0.1% Sodium azide in PBS). Data acquisition was on a FACSCalibur (BD Biosciences) using CellQuest version 3.3 (BD Biosciences). Analyses and calculation of median fluorescence intensity (MFI) was undertaken using FCS Express version 3.00.007 (Thornhill, Ontario, Canada).

Chromium Release Assay

The cytolytic activity of T cells was determined in a standard 4-hour chromium release assay (CRA) as described previously (5, 18).

Intracellular IFN-γ Production

10^5 T cells were incubated with 0.5×10^6 stimulator cells in 200 μL culture media along with protein transport inhibitor (BD Golgi Plug containing Brefeldin A, Cat# 555028) in a round-bottom 96-well plate. Following a 4 to 6 hour incubation at 37°C, the cells were stained for expression of CAR at 4°C for 30 minutes. After washing, the cells were fixed, permeabilized (for 20 min at 4°C with 100 μL of Cytofix/Cytoperm Buffer, Cat# 555028) and stained with APC-conjugated mAb specific for IFN-γ. Cells were further washed and analyzed by FACSCalibur. T cells treated with a Leukocyte activation cocktail (PMA and Ionomycin, Cat# 550583, BD Biosciences) were used as a positive control.

Induction of STAT3 phosphorylation

10^6 CAR^+ T cells were incubated with and without aAPC for 30 minutes at 37°C in a V-bottom 96-well plate. The cells were then fixed with 20 excess volumes of 37°C pre-warmed 1xPhosFlow Lyse/Fix Buffer (Cat# 558049, BD Biosciences) diluted in water at 37°C for 10 minutes to prevent dephosphorylation. Thereafter, pelleted cells were permeabilized by adding BD PhosFlow Perm Buffer III (Cat# 55850, BD Biosciences) for 20 minutes on ice, followed by washing with BD Pharmingen Staining Buffer (Cat# 554656). Resuspended

cells were then stained with antibodies for pSTAT3, CD3, and CAR for 20 minutes in the dark, washed once with BD Pharmingen Staining Buffer, and resuspended in the same buffer for flow cytometry analysis.

nCounter Analysis digital gene-expression system

Genetically modified T cells (10,000) were lysed in RNeasy Lysis Buffer (RLT) (5μL, Qiagen) and frozen for single-use aliquots at −80°C. Lysates were thawed and the selected mRNA content analyzed using the nCounter Analysis System (Model #NCT-SYST-120, NanoString Technologies, Seattle, WA) (19) after hybridization with a designer reporter code set and capture probe set for 12 hours at 65°C. The probes were designed, synthesized and hybridized using the nCounter Gene Expression Assay Kit. The post-hybridization processing was undertaken using the nCounter Prep Station. Nanominer software was used to perform normalization compared to internal control and basic statistical analysis on the data. The normalized results are expressed as the relative mRNA level.

In vivo efficacy of CAR$^+$ T cells

On day 0, seven-week-old NOD.Cg-*Prkdc*^{scid} *Il2rg*^{tm1Wjl}/SzJ (NSG) mice were intravenously (i.v.) injected via a tail vein with 10^5 GFP$^+$effLuc$^+$ NALM-6 cells. Mice (n = 5/group) in the two treatment cohorts received via tail vein injection (on days 1 and 9) 2×10^7 of CAR$^+$ T cells grown in the presence of IL-2 or CAR$^+$ T cells grown in the presence of IL-2 and IL-21. One group of mice (n=5) bearing tumor received no T cells. Anesthetized mice underwent bioluminescent imaging (BLI) in an anterior-posterior position using a Xenogen IVIS 100 series system (Caliper Life Sciences, Hopkinton, MA) 10 minutes after subcutaneous injection (at neck and shoulder) of 150 μL (200 μg/mouse) freshly thawed aqueous solution of D-Luciferin potassium salt (Caliper Life Sciences) as previously described (20). Photons emitted from NALM-6 xenografts were serially quantified using the Living Image 2.50.1 (Caliper Life Sciences) program. At the end of the experiment, mice were euthanized and tissues harvested. Bone marrow was flushed from the femurs using 30G×½inch needles (BD, Cat# 305106) with 2% FBS in PBS. Spleens were disrupted using a syringe in 2% FBS/PBS and passed through a 40 μm nylon cell strainer (BD, cat #352340) to obtain single cell suspension. Red blood cells from bone marrow, spleen, and peripheral blood were lysed using ACK lysing buffer (Gibco-Invitrogen, A10492) and remaining cells stained for presence of tumor (CD19 and GFP) by flow cytometry. Statistical analysis of photon flux and tumor burden was accomplished using Student's t-test.

RESULTS

Propagation of CAR$^+$ T cells with IL-21

A master cell-bank of clinical-grade K562-derived aAPC, designated clone #4, has been generated through the Production Assistance for Cellular Therapies (PACT) to propagate CAR$^+$ T cells to clinically-sufficient numbers. These γ-irradiated aAPC selectively propagate CAR$^+$ T cells after the electro-transfer of SB plasmids coding for CD19RCD28 CAR (5). To investigate extrinsic factors that might improve the therapeutic potential of CAR$^+$ T cells, a role for IL-21 was examined in the culturing process on aAPC. We added this soluble cytokine, in addition to soluble IL-2 and mIL-15 on aAPC, and demonstrated selective expansion of CAR$^+$ T cells (Figure 2A). This resulted in a greater number CD3$^+$ and CAR$^+$ T cells at 28 days of co-culture on clone #4 ($p<0.05$) compared with T cells receiving IL-2 alone, with differences between the two groups already apparent within 2 weeks after electroporation (Figure 2B,C). Indeed, the average fold expansion of CAR$^+$ T cells at 7 (2.75 ± 1.1 fold, n=7) and 14 (39.2 ± 36.2 fold, n=7) days after electroporation were significantly higher ($p<0.05$) compared to T-cells that only received IL-2 (day 7, 0.29 ± 0.3 fold, n=4; day 14, 0.49 ± 0.36 fold, n=4). After 4 weeks of co-culture on aAPC, the

group that received IL-21 had an average 19,800 ± 11,313 (n=7) fold expansion of $CD3^+$ T cells and there was a 35,800 ± 23,285 (n=7) fold expansion of CAR^+ T cells. In contrast, T cells that only received IL-2 had an average $CD3^+$ fold expansion of 2,280 ± 4,227 (n=4) and CAR^+ T cells expanded by an average of 2,680 ± 4,919 (n=4) fold. The average total cell numbers at 7 (4.1×10^7 vs. 4.7×10^6) and 14 (3.1×10^8 vs. 2.7×10^7) days after electroporation were significantly higher ($p<0.05$) in cultures receiving IL-21, as compared to cultures receiving only IL-2, which was due to an increased average number of average $CD3^+$ T cells (day 7, 4.1×10^7 vs. 3.0×10^6; day 14, 3.5×10^8 vs. 2.4×10^7; $p<0.05$). These data suggest the addition of IL-21 to the culture environment augments the propagation of $CD3^+CAR^+$ T cells on aAPC clone #4.

IL-21 results in qualitative differences in CAR^+ T cells

CAR^+ T cells cultured only in the presence of IL-2 produced low amounts of IFN-γ in response to CAR binding CD19 and expressed low levels of granzyme B. Expression of this cytokine and granzyme is associated with improved anti-tumor activity, therefore we investigated whether the presence of IL-21 could augment expression of these factors as T cells were propagated on aAPC. We measured mRNA levels using the nCounter Analysis System and IFN-γ and Granzyme B were found to be significantly elevated in populations of T cells receiving IL-21 (Figure 3A). At day 28 of culture, we observed a 3-fold increase in IFN-γ (313 vs. 100) and 40-fold increase in granzyme B (4,458 vs. 110) mRNA-transcript levels in T cells grown in IL-2 and IL-21, as compared to those grown in soluble IL-2. We demonstrated a significant increase in granzyme B protein levels (mean 89.5% vs. 17%) and CD19-dependent IFN-γ production (mean 55% vs. 0.1%) in the CAR^+ T cells receiving IL-21, as compared to those grown in soluble IL-2 (Figure 3B). Thus, the mRNA measurements are consistent with the phenotypic data showing an increase in expression of IFN-γ and granzyme B after co-culture of CAR^+ T cells with IL-2 and IL-21. We have previously generated CD19RCD28$^+$ T cells on $CD19^+$ aAPC in the presence of soluble IL-2 which tended to result in a preferential outgrowth of CAR^+ T cells with a predominance of $CD4^+$ T cells (5). Recognizing that $CD8^+$ T cells contribute to anti-tumor immunity, we sought a method to improve the outgrowth of $CD8^+CAR^+$ T cells on aAPC. IL-21 has been demonstrated to help propagate $CD8^+$ effector T cells (21), therefore the genetically modified T cells were co-cultured with aAPC in the presence of exogenous IL-21 and IL-2 for 28 days which resulted in a trend towards improved outgrowth of $CD8^+CAR^+$ compared with $CD4^+CAR^+$ T cells. Day 28 was selected as an endpoint for tissue culture and subsequent analyses since over this time period CAR^+ T cells expand to numbers sufficient for clinical translation (Figure 2). The T cells receiving IL-21 had 1.8-fold higher number of average $CD8^+$ T cells (24.2±25.3) compared to the T cells receiving just IL-2 (13.4±0.9) at day 28 of co-culture (Figure 3D). At the time of analysis, there was increased CAR expression on the T cells exposed to IL-21 compared to T cells cultured with only IL-2 (mean 90% ± 7.5 vs. 66% ± 7; $p<0.01$) which indicates that manipulating the cytokine milieu can improve the outgrowth of T cells with increased expression of CAR (Figure 3C). In aggregate, the addition of IL-21 compared to culturing only with IL-2, results in T cells containing sub-populations that have improved effector function, a trend towards $CD8^+$ phenotype, and augmented CAR expression.

IL-21 results in propagation of subpopulations of CAR^+ T cells with memory and naïve phenotypes

T cells propagated over a prolonged time in tissue culture tend to mature to a differentiated phenotype which may compromise their therapeutic potential. To determine if IL-21 can curtail this differentiation of genetically modified T cells, we examined the expression of (i) eomesodermin (Eomes) which controls cytolytic development and function of T cells, and has recently been shown to be reduced in naïve derived effector cells (22-24), and (ii) killer

cell lectin-like receptor subfamily G, member 1 (KLRG1), an inhibitory receptor that is expressed by senescent T cells (25, 26). At day 28, the T cells cultured only with IL-2 had increased levels of mRNA species coding for EOMES and KLRG1 demonstrating that this cytokine promoted differentiation of CAR^+ T cells on aAPC. However, when IL-21 was added there was a 7-fold and 54-fold reduction in EOMES and KLRG1, respectively (Figure 3A). To expand on the mRNA data, we examined the cell surface expression for flow cytometry markers of naïve, memory, and differentiated T cells. A naïve phenotype was defined by the presence of CD62L and CD45RA, whereas a central memory phenotype can be defined by the expression of CD28, CD62L, CCR7, and CD45RO on T cells (27-29). Differentiated effector cells typically lose expression of these markers upon prolonged culturing and exhausted cells upregulate expression of PD-1 and PDL-1 (30). CAR^+ T cells grown in the presence of IL-2 and IL-21 exhibited markers consistent with both naïve and memory cells and lacked expression of PD-1/PDL-1 (Figure 4A). In addition, the lack of (2%) CD57 expression supports absence of exhaustion among the CAR^+ T cells (31). At day 28 of culture, the CAR^+ T cells expressed CD28 (mean 69%, range 22-88%), CCR7 (mean 16%, range 0.9-60.5%), CD62L (mean 50%, range 22-75%), CD45RO (93%, range 84-98%) and IL7Rα (mean 26%, range 9-37). Among the CAR^+ cells were T cells with a central memory phenotype (T_{CM}) exemplified by the co-expression of $CD28^+CD62L^+$ (34%, range 11 - 59%), $CD28^+CCR7^+$ (mean 18%, range 0.8 - 56.5%), $CD62L^+$,$CCR7^+$ (10%, range 0.5 - 48%), $CD45RO^+CD45RA^+$ (mean 19%, range 2 - 63%). In summary, the addition of IL-21 supports the numeric expansion of CAR^+ T cells on aAPC that contain memory and naïve sub-populations.

Redirected specificity of CAR^+ T cells numerically expanded with IL-21

T cells expressing CAR and propagated in the presence of IL-2 and IL-21 were able to specifically lyse $CD19^+$ tumor targets (Figure 4B). At an effector:target ratio of 5:1, the CAR^+ T cells could lyse an average 51% (range 32 - 66%) of $CD19^+$ Daudiβ_2m cells and an average 38% (range 25 - 60%) of $CD19^+$ NALM-6. The Daudi cells used as targets were genetically modified to express β_2 microglobulin and thus re-express classical HLA class I (Supplementary Figure 1) to decrease unwanted killing by contaminating NK or lymphokine-activated killer cells. Specificity for CD19 was demonstrated by a 4.5-fold (range 1.3 - 12.6) increased killing of genetically modified $CD19^+$ U251T (glioma) targets as compared to parental $CD19^{neg}$ U251T targets at an effector:target ratio of 5:1. We further assessed the function of CAR^+ T cells by evaluating their ability to produce IFN-γ in response to CD19 (Figure 4C). When CAR^+ T cells were stimulated with $CD19^+$ Daudiβ_2m cells there was an average 29.6-fold (range 4.6 - 114.9) increase in IFN-γ production. The specificity for production of CD19 was demonstrated by a 12.6-fold (range 3.2 - 45.5) increase in IFN-γ production by CAR^+ T cells when co-cultured with $CD19^+$ U251T cells in comparison to $CD19^{neg}$ U251T cells. These data demonstrate that CAR^+ T cells cultured in the presence of IL-21 exhibit CD19-dependent redirected effector functions.

Efficacy of CAR^+ T cells propagated on aAPC to treat B-lineage malignancy

We investigated whether CAR^+ T cells numerically expanded in the presence of IL-2 and IL-21 were able to demonstrate an improved anti-tumor effect compared with CAR^+ T cells cultured with only IL-2. Mice injected with NALM-6 were longitudinally measured by BLI for tumor-associated ffLuc activity. We observed that CAR^+ T cells grown in the presence of IL-2 and IL-21 were more effective in controlling tumor growth as compared to CAR^+ T cells grown in the presence of IL-2 (day 8, $p<0.01$; day 13, $p<0.05$; day 17, $p<0.05$) and as compared to mice that did not receive T cells (days 8, 13, 17, $p<0.01$) (Figure 5 A and B). Groups of mice receiving no T cells or CAR^+ T cells grown in the presence of IL-2 showed similar rates of tumor growth (day 8, $p=0.11$; day 13, $p=0.2$; day 17, $p=0.07$). Tissues from mice were assessed for GFP^+CD19^+ NALM-6 and consistent with the BLI data, we

observed the tumor burden was significantly reduced in mice receiving CAR^+ T cells grown in the presence of IL-2 and IL-21, as compared to mice receiving no T cells or CAR^+ T cells grown in the presence of IL-2 (Figure 5C and D). The presence of NALM-6 blasts in peripheral blood was lower in the IL-2 and IL-21 (1.8 ± 0.92, mean ± standard deviation, SD) group as compared to mice that received CAR^+ T cells cultured with IL-2 (20.4 ± 20.3, $p<0.05$) or no T cells (3.8 ± 0.6, $p<0.01$). There was also a significant reduction in average tumor burden in the bone marrow after administration of T cells that were cultured with IL-2 and IL-21 group (48.5 ± 4.2) as compared to IL-2 group (86.6 ± 7.8, $p<0.00001$) or no T-cell group (86.6 ± 7.9, $p<<0.001$). The difference in average splenic tumor burden was more apparent ($p<0.0001$) comparing mice that received CAR^+ T cells cultured with IL-2 and IL-21 (30.9 ± 18.8) vs. mice that were infused with CAR^+ cells cultured with IL-2 (88.3 ± 4). The tumor burden was similar in the blood ($p = 0.07$) and bone marrow ($p = 0.49$) between the mice that received no T cells and mice that received CAR^+ T cells cultured with IL-2. Thus, these *in vivo* data confirm that CD19-specific CAR^+ cells propagated on aAPC in presence of IL-2 and IL-21 are superior in controlling tumor growth.

A membrane bound mutein of IL-21 can replace soluble recombinant IL-21

Signaling through CAR and cytokine receptor(s) occurs in the tissue culture environment enabling aAPC to selectively propagate T cells that receive signals 1, 2 and 3. To improve the coordination between these signals, we altered the aAPC to not only provide the CD19 antigen and associated co-stimulatory molecules, but to express a novel mutein of membrane-bound of IL-21 (Figure 6A). This enabled us to test the hypothesis that expressing IL-21 on the cell surface of the aAPC could replace the need for providing IL-21 as a soluble recombinant cytokine. To accomplish this, the aAPC clone #4 were electroporated with the SB plasmid $_{CoOp}$IL-21-Fc/pT-MNDU3 and a sub-clone (D2) was selected based on uniform expression of mIL-21 and the other introduced cell surface markers (Figure 6B). PBMC electroporated with SB system to express CD19RCD28 and propagated on γ-irradiated $mIL\text{-}21^+$ aAPC in the absence of soluble IL-21, but in the presence of soluble IL-2, resulted in an outgrowth of CAR^+ T cells (Figure 7A). The CAR expression (81% vs. 79%) was similar to when T cells were grown in the presence of exogenous IL-21 or with aAPC expressing mIL-21. The average fold expansion at the end of 28 days of co-culture as assessed by expression of CD3 (11,700; $p = 0.27$, not significant NS) and CAR (14,000; $p = 0.17$, NS) on T cells numerically expanded with $mIL\text{-}21^+$ aAPC was similar to the T cells propagated with soluble IL-21 (Figure 7B). The CAR^+ T cells numerically expanded on $mIL\text{-}21^+$ aAPC demonstrated specific lysis of $CD19^+$ target cells and a 13-fold increase in IFN-γ production when cells were stimulated with $CD19^+$ U251T targets over control $CD19^{neg}$U251T cells (Figure 7D). To examine if mIL-21 can directly activate T cells, we evaluated the phosphorylation status of STAT3. CAR^+ T cells that were propagated for 28 days with IL-2 plus $mIL\text{-}21^{neg}$ aAPC (clone #4) and IL-2 plus $mIL\text{-}21^+$ aAPC (clone #D2), were stimulated for 30 minutes on aAPC with (clone #D2) or without mIL-21 (clone #4). T cells cultured with IL-2 and soluble IL-21 stimulated with aAPC (clone #4) along with soluble IL-21 were used as positive controls. CAR^+ T cells cultured on $mIL\text{-}21^+$ aAPC in the presence of IL-2 when then stimulated with $mIL\text{-}21^+$ aAPC resulted in an increase in MFI of pSTAT3 (27.1), over the unstimulated control T cells (11.6), or when stimulated with aAPC lacking mIL-21 (13.2) (Figure 7C). When CAR^+ T cells which had been propagated on aAPC (clone #4) in the presence of IL-2 (and had not seen IL-21 in any form) were exposed to $mIL\text{-}21^+$ aAPC, there was a similar increase in MFI of pSTAT3 (25.2) compared to the controls (unstimulated, 11.1; aAPC lacking mIL-21, 14.3). These data demonstrate that mIL-21 on aAPC is functional and capable of activating T cells through the STAT3 pathway. In aggregate, these data suggest that $mIL\text{-}21^+$ aAPC can replace soluble recombinant IL-21 to selectively propagate CAR^+ T cells with redirected specificity.

DISCUSSION

The tissue culture environment can be modified to play a critical role in the growth and function of T cells propagated *in vitro*. In the current study, we demonstrate that the addition of IL-21 to the culture milieu in soluble form or presented in conjunction with antigen on aAPC results in improved effector function and preservation of naïve/memory phenotype of CAR^+ T cells which predicts for improved therapeutic effect in clinical trials.

Initial (first generation) CARs typically linked a scFv to a single signaling moiety (e.g. CD3-ζ) and these typically demonstrated a lack of sustained persistence *in vivo* (2). Therefore, the CAR design was modified to add one or more co-stimulatory signaling domains of CD28 (4), 4-1BB (32, 33), OX40 (34) to generate “second” or, “third” generation CARs. We have previously described our second generation CAR, CD19RCD28, which provides CD19-dependent signaling through CD3ζ and CD28 resulting in improved persistence and anti-tumor effect (4). Operating under the premise that T cells propagated in a CAR-dependent manner *ex vivo* may select for T cells with sustained proliferation *in vivo*, we developed a culturing system based on aAPC to selectively numerically expand CAR^+ T cells. Such aAPC derived from K562 can be tailored to express cell-surface antigen (35) or intracellular antigen presented by restricting MHC (36, 37) in the context of desired and introduced T-cell co-stimulatory molecules (37-40). Our aAPC (clone #4) were also engineered to express mIL-15 and this membrane-bound cytokine is present throughout our culturing process in addition to the addition of soluble cytokines. The addition of IL-21-mediated signaling during the culturing process to selectively propagate T cells expressing a second generation CD19-specific CAR resulted in an outgrowth of T cells on aAPC with a desired phenotype and improved function when assessed *in vitro* and *in vivo*. Thus, from the perspective of manufacturing CAR^+ T cells for clinical application it appears beneficial to include IL-21 in the culturing process.

It has been previously demonstrated that the tissue culture microenvironment can be altered with cytokines for improved T-cell function. For example, T cells can be primed using cytokines to augment immune responses after adoptive transfer. In some cases, this is dependent on generation of memory phenotype which requires the presence of IL-15 and IL-21 (41, 42). This memory phenotype predicts for improved persistence as demonstrated for T cells cultured with IL-7, IL-15, and IL-21, compared to T cells propagated with IL-2 (8, 43, 44). Our paper provides supportive evidence that not only can the CAR be manipulated, but the choice of additional cytokines influences the number and character of the propagated CAR^+ T cells.

Membrane bound cytokines (45, 46) offer an attractive approach for delivering a desired cytokine to the immediate microenvironment of the T cell-aAPC synapse along with alleviating the need to add the soluble (expensive) cytokine to the culture system and avoiding the need for a clinical-grade cytokine for clinical applications. Membrane-bound IL-15 has been used to propagate T cells (6, 47) and NK cells (48, 49) on aAPC derived from K562 cells. Our aAPC (clone #4) used in this study expresses mIL-15 and is being used in our clinical trials infusing patient- and donor-derived CD19-specific CAR^+ T cells after autologous and allogeneic hematopoietic stem-cell transplantation. Building upon the success of aAPC expressing mIL-15, we further modified the aAPC to co-express mIL-21 and suggest that this genetic approach to aAPC design may avoid the need to add soluble recombinant IL-21 to the culture.

Our data demonstrate that the SB system and aAPC platform can be manipulated to culture T cells to receive three coordinated signals. This was achieved by influencing intrinsic (CAR) and now extrinsic (tissue culture) factors to improve the therapeutic potential of

genetically modified and propagated T cells. Activation through 2nd generation CAR, triggered by CD3ζ (signal 1) and CD28 (signal 2), and common γ_c receptor (triggered by IL-21, signal 3) results in generation of CAR^+ T cells that have an improved ability to respond to CD19 compared to T cells cultured without IL-21. The ability to augment signal 3 leads to an outgrowth of CAR^+ T cells on aAPC that have desired properties for use in clinical trials.

Supplementary Material

Refer to Web version on PubMed Central for supplementary material.

Acknowledgments

Support from: Cancer Center Core Grant (CA16672); DOD PR064229; PO1 (CA100265); RO1 (CA124782, CA120956, CA141303); R33 (CA116127); Mr. and Mrs. Joe H. Scales; The Alex Lemonade Stand Foundation; The Burroughs Wellcome Fund; The Cancer Prevention Research Institute of Texas; The Gillson Longenbaugh Foundation; The Harry T. Mangurian, Jr., Foundation, The Institute of Personalized Cancer Therapy; The Leukemia and Lymphoma Society; The Lymphoma Research Foundation; The Miller Foundation; The National Foundation for Cancer Research; The Pediatric Cancer Research Foundation; The William Lawrence and Blanche Hughes Children's Foundation.

We thank Karen Ramirez and David He from Flow Cytometry Core Laboratory (NIH grant # 5P30CA016672-32) for their help with flow cytometry. We thank Brian Rabinovich for assistance with transduction of NALM-6 tumor cells.

REFERENCES

1. Jensen MC, Popplewell L, DiGiusto DL, Kalos M, Cooper LJN, Raubitschek A, Forman SJ. A first-in-human clinical trial of adoptive therapy using CD19-specific chimeric antigen receptor re-directed T cells for recurrent/refrctory follicular lymphoma. Molecular Therapy. 2007; 15:S142.
2. Jensen MC, Popplewell L, Cooper LJ, et al. Antitransgene rejection responses contribute to attenuated persistence of adoptively transferred CD20/CD19-specific chimeric antigen receptor redirected T cells in humans. Biol Blood Marrow Transplant. 16:1245–56. [PubMed: 20304086]
3. Jena B, Dotti G, Cooper LJ. Redirecting T-cell specificity by introducing a tumor-specific chimeric antigen receptor. Blood. 116:1035–44. [PubMed: 20439624]
4. Kowolik CM, Topp MS, Gonzalez S, et al. CD28 costimulation provided through a CD19-specific chimeric antigen receptor enhances in vivo persistence and antitumor efficacy of adoptively transferred T cells. Cancer Res. 2006; 66:10995–1004. [PubMed: 17108138]
5. Singh H, Manuri PR, Olivares S, et al. Redirecting specificity of T-cell populations for CD19 using the Sleeping Beauty system. Cancer Res. 2008; 68:2961–71. [PubMed: 18413766]
6. Davies JK, Singh H, Huls H, et al. Combining CD19 redirection and alloanergization to generate tumor-specific human T cells for allogeneic cell therapy of B-cell malignancies. Cancer Res. 70:3915–24. [PubMed: 20424114]
7. Hackett PB, Largaespada DA, Cooper LJ. A transposon and transposase system for human application. Mol Ther. 18:674–83. [PubMed: 20104209]
8. Moroz A, Eppolito C, Li Q, Tao J, Clegg CH, Shrikant PA. IL-21 enhances and sustains CD8+ T cell responses to achieve durable tumor immunity: comparative evaluation of IL-2, IL-15, and IL-21. J Immunol. 2004; 173:900–9. [PubMed: 15240677]
9. Ma HL, Whitters MJ, Konz RF, et al. IL-21 activates both innate and adaptive immunity to generate potent antitumor responses that require perforin but are independent of IFN-gamma. J Immunol. 2003; 171:608–15. [PubMed: 12847225]
10. Brady J, Hayakawa Y, Smyth MJ, Nutt SL. IL-21 induces the functional maturation of murine NK cells. J Immunol. 2004; 172:2048–58. [PubMed: 14764669]
11. Casey KA, Mescher MF. IL-21 promotes differentiation of naive CD8 T cells to a unique effector phenotype. J Immunol. 2007; 178:7640–8. [PubMed: 17548600]

12. Markley JC, Sadelain M. IL-7 and IL-21 are superior to IL-2 and IL-15 in promoting human T cell-mediated rejection of systemic lymphoma in immunodeficient mice. Blood. 115:3508–19. [PubMed: 20190192]
13. Hashmi MH, Van Veldhuizen PJ. Interleukin-21: updated review of Phase I and II clinical trials in metastatic renal cell carcinoma, metastatic melanoma and relapsed/refractory indolent non-Hodgkin's lymphoma. Expert Opin Biol Ther. 10:807–17. [PubMed: 20384523]
14. Li Y, Yee C. IL-21 mediated Foxp3 suppression leads to enhanced generation of antigen-specific CD8+ cytotoxic T lymphocytes. Blood. 2008; 111:229–35. [PubMed: 17921346]
15. Manuri PV, Wilson MH, Maiti SN, et al. piggyBac transposon/transposase system to generate CD19-specific T cells for the treatment of B-lineage malignancies. Hum Gene Ther. 21:427–37. [PubMed: 19905893]
16. Serrano LM, Pfeiffer T, Olivares S, et al. Differentiation of naive cord-blood T cells into CD19-specific cytolytic effectors for posttransplantation adoptive immunotherapy. Blood. 2006; 107:2643–52. [PubMed: 16352804]
17. Rabinovich BA, Ye Y, Etto T, et al. Visualizing fewer than 10 mouse T cells with an enhanced firefly luciferase in immunocompetent mouse models of cancer. Proc Natl Acad Sci U S A. 2008; 105:14342–6. [PubMed: 18794521]
18. Cooper LJ, Topp MS, Serrano LM, et al. T-cell clones can be rendered specific for CD19: toward the selective augmentation of the graft-versus-B-lineage leukemia effect. Blood. 2003; 101:1637–44. [PubMed: 12393484]
19. Geiss GK, Bumgarner RE, Birditt B, et al. Direct multiplexed measurement of gene expression with color-coded probe pairs. Nat Biotechnol. 2008; 26:317–25. [PubMed: 18278033]
20. Singh H, Serrano LM, Pfeiffer T, et al. Combining adoptive cellular and immunocytokine therapies to improve treatment of B-lineage malignancy. Cancer Res. 2007; 67:2872–80. [PubMed: 17363611]
21. Li Y, Bleakley M, Yee C. IL-21 influences the frequency, phenotype, and affinity of the antigen-specific CD8 T cell response. J Immunol. 2005; 175:2261–9. [PubMed: 16081794]
22. Pearce EL, Mullen AC, Martins GA, et al. Control of effector CD8+ T cell function by the transcription factor Eomesodermin. Science. 2003; 302:1041–3. [PubMed: 14605368]
23. Intlekofer AM, Takemoto N, Wherry EJ, et al. Effector and memory CD8+ T cell fate coupled by T-bet and eomesodermin. Nat Immunol. 2005; 6:1236–44. [PubMed: 16273099]
24. Hinrichs CS, Borman ZA, Gattinoni L, et al. Human effector CD8+ T cells derived from naive rather than memory subsets possess superior traits for adoptive immunotherapy. Blood. 117:808–14. [PubMed: 20971955]
25. Henson SM, Franzese O, Macaulay R, et al. KLRG1 signaling induces defective Akt (ser473) phosphorylation and proliferative dysfunction of highly differentiated CD8+ T cells. Blood. 2009; 113:6619–28. [PubMed: 19406987]
26. Voehringer D, Koschella M, Pircher H. Lack of proliferative capacity of human effector and memory T cells expressing killer cell lectinlike receptor G1 (KLRG1). Blood. 2002; 100:3698–702. [PubMed: 12393723]
27. Dutton RW, Bradley LM, Swain SL. T cell memory. Annu Rev Immunol. 1998; 16:201–23. [PubMed: 9597129]
28. Sallusto F, Lenig D, Forster R, Lipp M, Lanzavecchia A. Two subsets of memory T lymphocytes with distinct homing potentials and effector functions. Nature. 1999; 401:708–12. [PubMed: 10537110]
29. Sallusto F, Geginat J, Lanzavecchia A. Central memory and effector memory T cell subsets: function, generation, and maintenance. Annu Rev Immunol. 2004; 22:745–63. [PubMed: 15032595]
30. Barber DL, Wherry EJ, Masopust D, et al. Restoring function in exhausted CD8 T cells during chronic viral infection. Nature. 2006; 439:682–7. [PubMed: 16382236]
31. Brenchley JM, Karandikar NJ, Betts MR, et al. Expression of CD57 defines replicative senescence and antigen-induced apoptotic death of CD8+ T cells. Blood. 2003; 101:2711–20. [PubMed: 12433688]

32. Imai C, Andreansky M, et al. Chimeric receptors with 4-1BB signaling capacity provoke potent cytotoxicity against acute lymphoblastic leukemia. Leukemia. 2004; 18:676–84. MK. [PubMed: 14961035]
33. Brentjens RJ, Santos E, Nikhamin Y, et al. Genetically targeted T cells eradicate systemic acute lymphoblastic leukemia xenografts. Clin Cancer Res. 2007; 13:5426–35. [PubMed: 17855649]
34. Pule MA, Dotti G, et al. A chimeric T cell antigen receptor that augments cytokine release and supports clonal expansion of primary human T cells. Mol Ther. 2005; 12:933–41. SK. [PubMed: 15979412]
35. Numbenjapon T, Serrano LM, Singh H, et al. Characterization of an artificial antigen-presenting cell to propagate cytolytic CD19-specific T cells. Leukemia. 2006; 20:1889–92. [PubMed: 17041638]
36. Latouche JB, Sadelain M. Induction of human cytotoxic T lymphocytes by artificial antigen-presenting cells. Nat Biotechnol. 2000; 18:405–9. [PubMed: 10748520]
37. Hirano N, Butler MO, Xia Z, et al. Efficient presentation of naturally processed HLA class I peptides by artificial antigen-presenting cells for the generation of effective antitumor responses. Clin Cancer Res. 2006; 12:2967–75. [PubMed: 16707591]
38. Maus MV, Thomas AK, Leonard DG, et al. Ex vivo expansion of polyclonal and antigen-specific cytotoxic T lymphocytes by artificial APCs expressing ligands for the T-cell receptor, CD28 and 4-1BB. Nat Biotechnol. 2002; 20:143–8. [PubMed: 11821859]
39. Suhoski MM, Golovina TN, Aqui NA, et al. Engineering artificial antigen-presenting cells to express a diverse array of co-stimulatory molecules. Mol Ther. 2007; 15:981–8. [PubMed: 17375070]
40. Hirano N, Butler MO, Xia Z, et al. Engagement of CD83 ligand induces prolonged expansion of CD8+ T cells and preferential enrichment for antigen specificity. Blood. 2006; 107:1528–36. [PubMed: 16239433]
41. Neeson P, Shin A, Tainton KM, et al. Ex vivo culture of chimeric antigen receptor T cells generates functional CD8+ T cells with effector and central memory-like phenotype. Gene Ther. 17:1105–16. [PubMed: 20428216]
42. Zeng R, Spolski R, Finkelstein SE, et al. Synergy of IL-21 and IL-15 in regulating CD8+ T cell expansion and function. J Exp Med. 2005; 201:139–48. [PubMed: 15630141]
43. Hinrichs CS, Spolski R, Paulos CM, et al. IL-2 and IL-21 confer opposing differentiation programs to CD8+ T cells for adoptive immunotherapy. Blood. 2008; 111:5326–33. [PubMed: 18276844]
44. Schluns KS, Lefrancois L. Cytokine control of memory T-cell development and survival. Nat Rev Immunol. 2003; 3:269–79. [PubMed: 12669018]
45. Kim YS. Tumor Therapy Applying Membrane-bound Form of Cytokines. Immune Netw. 2009; 9:158–68. [PubMed: 20157604]
46. Cimino AM, Palaniswami P, Kim AC, Selvaraj P. Cancer vaccine development: protein transfer of membrane-anchored cytokines and immunostimulatory molecules. Immunol Res. 2004; 29:231–40. [PubMed: 15181285]
47. Wu Z, Xu Y. IL-15R alpha-IgG1-Fc enhances IL-2 and IL-15 anti-tumor action through NK and CD8+ T cells proliferation and activation. J Mol Cell Biol. 2:217–22. [PubMed: 20671116]
48. Fujisaki H, Kakuda H, Imai C, Mullighan CG, Campana D. Replicative potential of human natural killer cells. Br J Haematol. 2009; 145:606–13. [PubMed: 19344420]
49. Gong W, Xiao W, Hu M, et al. Ex vivo expansion of natural killer cells with high cytotoxicity by K562 cells modified to co-express major histocompatibility complex class I chain-related protein A, 4-1BB ligand, and interleukin-15. Tissue Antigens.

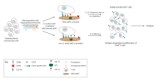

Figure 1. Generation of CAR$^+$ T cells on γ-irradiated aAPC

PBMC were electroporated with SB transposon (blue) and transposase (red). Cells were subsequently co-cultured on K562-derived aAPC [modified to co-express CD19, CD64, CD86, CD137L (4-1BBL), mIL-15, with and without mIL-21] in the presence of soluble IL-21 and/or IL-2.

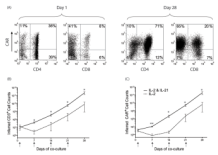

Figure 2. Propagation of genetically modified T cells on aAPC

(A) T-cell expression of CAR before and after propagation on aAPC. The rate of T-cell growth cultured on γ-irradiated aAPC for 28 days in the presence of IL-2 (n=4) or IL-2 and IL-21 (n=7). The total number of (B) $CD3^+$ cells, and (C) CAR^+ T cells propagated over time. Small arrows indicate the addition of γ-irradiated aAPC to the culture. Inferred cell counts were calculated assuming all viable cells were carried forward through each stimulation cycle. Mean±SD is shown, * $p<0.05$; ** $p<0.001$.

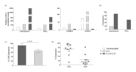

Figure 3. IL-21 supports outgrowth of T cells with improved CAR expression and desired phenotype

CAR^+ T cells grown in the presence of IL-2, or IL-21 and IL-2, at the end of 28 days of co-culture on aAPC were evaluated for: (A) The amount of mRNA transcripts coding for Granzyme B, IFN-γ, EOMES and KLRG1 using NanoString nCounter analysis, and (B) Expression of Granzyme B and CD19-specific IFN-γ (percent IFN-γ production when cells were stimulated with $CD19^+$U251T as compared to $CD19^{neg}$ U251T) using flow cytometry. (C) Total CAR expression (mean ± SD). (D) Percent CD4 and CD8 T cells in cultures receiving IL-2 and IL-2&IL-21 at the end of 28 days of co-culture over aAPC. Each circle represents individual experiment, horizontal bars represent mean expression, solid (IL-2 and IL-21) and dotted (IL-2).

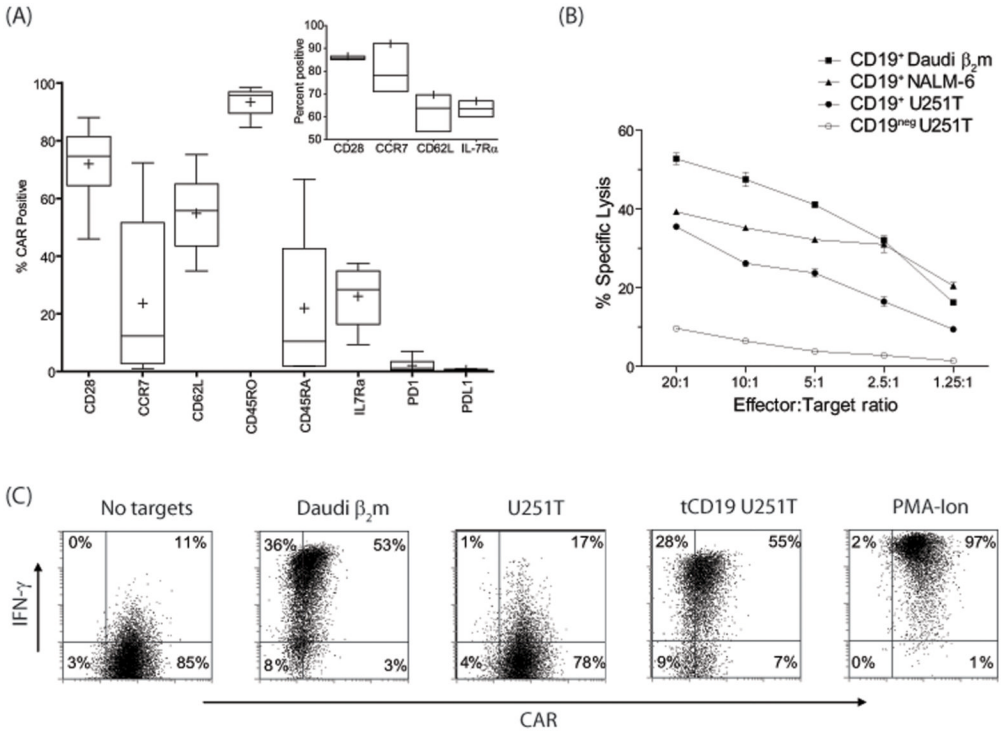

Figure 4. IL-21 supports outgrowth of sub-populations of naïve and memory CD19-specific CAR$^+$T cells

(A) Immunophenotype of genetically modified T cells numerically expanded in the presence of IL-2 and IL-21. Inset shows expression of selected cell-surface proteins before electroporation on T cells obtained from PBMC (n=3). Data are presented as 'Box-and-Whiskers' plot and in inset as 'Low-high-bar' plot. Horizontal bar within boxes represents median and '+' represents mean value. (B) Four-hour CRA demonstrates killing of CD19$^+$ Daudiβ_2m, NALM-6, and CD19$^+$U251T cells. Lysis of CD19^{neg}U251T cells shows background killing. Mean±SD for triplicate wells is represented. (C) IFN-γ production by CAR$^+$ T cells upon incubation with targets. PMA-Ionomycin is used as a positive control.

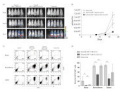

Figure 5. Efficacy of CAR$^+$ T cells in mice

NSG mice i.v. injected (day 0) with 10^5 GFP$^+$effLuc$^+$ NALM-6 tumor received, on days 1 and 9, 2×10^7 CAR$^+$ T cells grown in the presence of IL-2 or IL-2 & IL-21, or received no T cells. (A) False-colored images representing photon flux from NALM-6-derived ffLuc activity. (B) Time course of longitudinal measurements of tumor-derived mean photon flux ± SD from 3 groups of mice (n=5). Background luminescence (10^6 p/s/cm^2/sr) was defined from mice with no tumor imaged after receiving D-Luciferin in parallel with mice in treatment groups. *In vitro* ffLuc-derived activity of genetically modified GFP$^+$effLuc$^+$ NALM-6 was 2.8 ± 0.2 cpm/cell (mean ± SD) compared with 0.003 ± 0.001 cpm/cell (mean ± SD) for parental NALM-6 cells that do not express ffLuc. (C) At the end of the experiment (day 21) mice were euthanized and tissues (blood, bone marrow, spleen) were harvested and analyzed by flow cytometry for expression of CD19 and GFP. Representative flow cytometry dot plots for tumor at various sites are shown. (E) The percentage of CD19$^+$GFP$^+$ cells present in mice from the three groups (mean ± SD) is shown along with statistical significance (*p<0.05, **p<0.01).

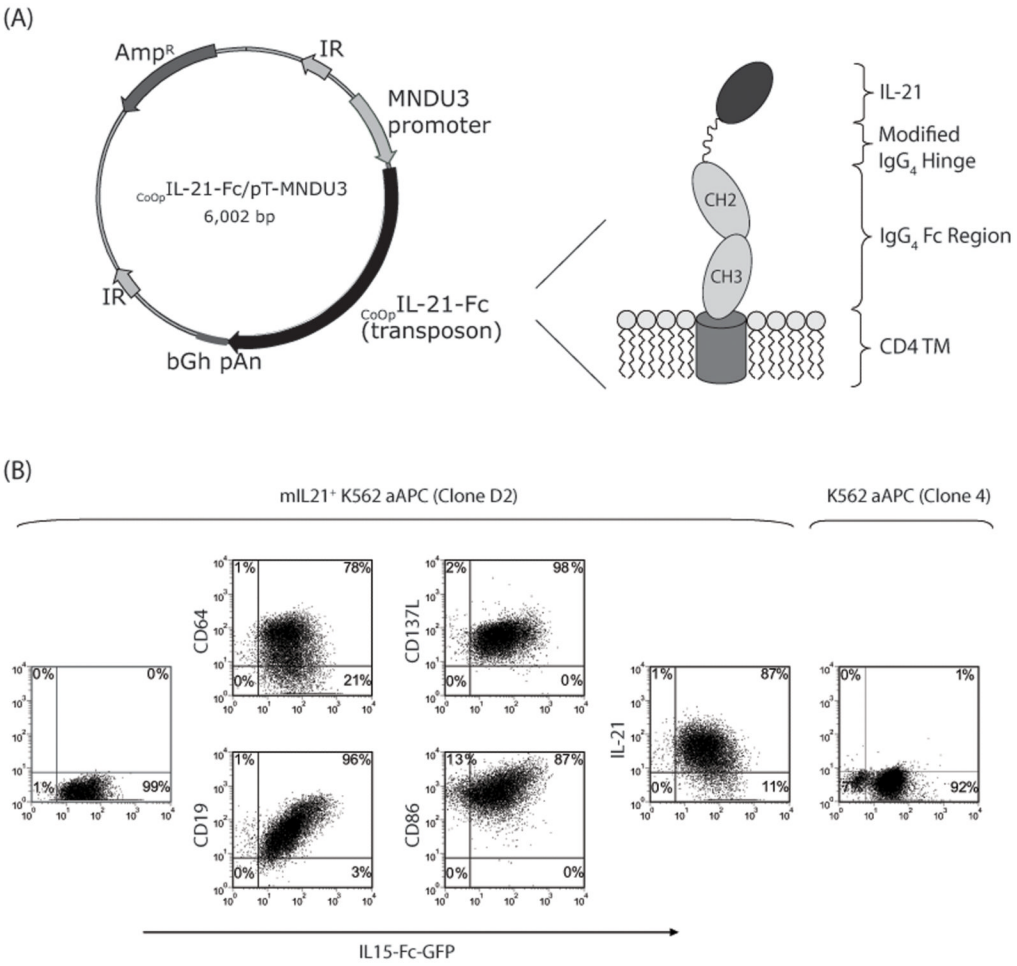

Figure 6. Expression of membrane-bound IL-21 (mIL-21)

(A) Schematic of the DNA plasmid, $_{CoOp}$IL-21-Fc/pT-MNDU3, expressing mIL-21 along with a cartoon showing the folded mIL-21 protein. Abbreviations: MNDU3 promoter, promoter from U3 region of the MND retrovirus; $_{CoOp}$IL-21-Fc, codono-ptimized mIL-21 (IL-21-Fc fusion); IR, SB-inverted/direct repeats; bGh pAn, polyadenylation signal from bovine growth hormone; Amp^R, ampicillin resistance gene. (B) Dot-plots showing the presence of mIL-21 (detected by mAb against IL-21) and cell surface markers (CD19, CD64, CD86, CD137, mIL-15) on the aAPC.

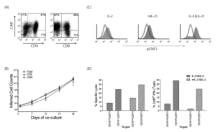

Figure 7. Characterization of T cells grown on mIL-21^{+} aAPC

(A) CAR expression on CD4^{+} and CD8^{+} T cells after 28 days of co-culture on mIL-21^{+} aAPC (clone#D2) along with exogenous IL-2. (B) Expansion of total, CD3^{+} and CAR^{+} T cells over 28 days of culture period. (C) Induction of STAT3 phosphorylation was measured in T cells grown with IL-2 or mIL-21 & IL-2. These propagated T cells were subsequently stimulated by aAPC with (Clone D2, filled grey histograms) or without (Clone 4, black histograms) mIL-21 for 30 minutes, then fixed, permeabilized, and stained for flow cytometry. Cells grown in presence of IL-2 and soluble IL-21 stimulated with aAPC (Clone 4) with (filled grey histogram) and without (black histogram) soluble IL-21 were used as control. Histograms (dotted, unstimulated cells) represent phosphoSTAT3 staining and indicate a shift in MFI. (D) Redirected specificity of CAR^{+} T cells grown on mIL-21^{+} aAPC with IL-2 as measured by 4-hour CRA and flow cytometry for IFN-γ production.